JCI insight

# WEE1 kinase is a therapeutic vulnerability in CIC-DUX4 undifferentiated sarcoma

Rovingaile Kriska M. Ponce, … , Tadashi Kondo, Ross A. Okimoto

*JCI Insight.* 2022;7(6):e152293. https://doi.org/10.1172/jci.insight.152293.

**Research Article** **Oncology**

## Graphical abstract

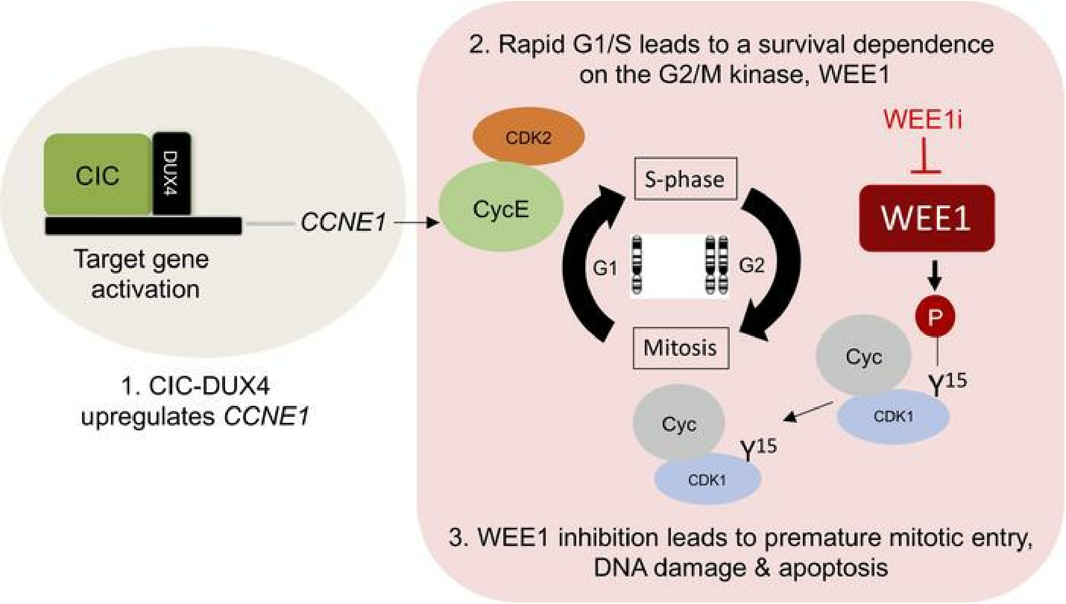
CIC
DUX4
CCNE1
Target gene activation
1. CIC-DUX4 upregulates *CCNE1*
2. Rapid G1/S leads to a survival dependence on the G2/M kinase, WEE1
CDK2
CycE
S-phase
G1
G2
Mitosis
WEE1i
WEE1
P
Cyc
Y15
CDK1
Cyc
Y15
CDK1
3. WEE1 inhibition leads to premature mitotic entry, DNA damage & apoptosis

**Find the latest version:**

https://jci.me/152293/pdf

JCI insight

# WEE1 kinase is a therapeutic vulnerability in CIC-DUX4 undifferentiated sarcoma

**Rovingaile Kriska M. Ponce,[1] Nicholas J. Thomas,[1] Nam Q. Bui,[2] Tadashi Kondo,[3] and Ross A. Okimoto[1,4]**

[1]Department of Medicine, UCSF, San Francisco, California, USA. [2]Department of Medicine, Stanford University School of Medicine, Stanford, California, USA. [3]Division of Rare Cancer Research, National Cancer Center Research Institute, Tokyo, Japan. [4]Helen Diller Family Comprehensive Cancer Center, UCSF, San Francisco, California, USA.

**CIC-DUX4 rearrangements define an aggressive and chemotherapy-insensitive subset of undifferentiated sarcomas. The CIC-DUX4 fusion drives oncogenesis through direct transcriptional upregulation of cell cycle and DNA replication genes. Notably, CIC-DUX4–mediated *CCNE1* upregulation compromises the $G_1$/S transition to confer a dependence on the $G_2$/M cell cycle checkpoint. Through an integrative transcriptional and kinase activity screen using patient-derived specimens, we now show that CIC-DUX4 sarcomas depend on the $G_2$/M checkpoint regulator WEE1 as part of an adaptive survival mechanism. Specifically, CIC-DUX4 sarcomas depended on WEE1 activity to limit DNA damage and unscheduled mitotic entry. Consequently, genetic or pharmacologic WEE1 inhibition in vitro and in vivo led to rapid DNA damage–associated apoptotic induction of patient-derived CIC-DUX4 sarcomas. Thus, we identified WEE1 as a vulnerability targetable by therapeutic intervention in CIC-DUX4 sarcomas.**

## Introduction

Chromosomal rearrangements that create transcription factor (TF) fusion oncoproteins are attractive cancer-specific therapeutic targets (1). For example, mechanistic studies that provide insight into fusion oncoprotein stability have led to the development of precision medicine–based therapies that directly degrade these driver oncoproteins (1–3). Beyond direct degradation, an alternative strategy to overcome TF fusion dependence in cancer is identification of key transcriptional targets directly controlled by TF fusions to drive malignant progression. To this end, we recently observed that CIC-DUX4 sarcoma is molecularly dependent on the CCNE/CDK2 complex: CIC-DUX4 acquires neomorphic function as a transcriptional activator to upregulate *CCNE1,* driving sarcoma growth and survival (4). Therapeutic intervention with CDK2 inhibitors leads to induction of apoptosis in models using patient-derived CIC-DUX4 samples (4). These findings provided a mechanism-based therapeutic strategy to limit CIC-DUX4 sarcoma progression, which remains an aggressive and lethal disease.

In other cancers, increased expression of *CCNE1* through transcriptional upregulation or amplification often leads to a deficient $G_1$/S checkpoint, thus enhancing DNA replication stress and genomic instability (5–11). Cancer cells adapt to these high-replication-stress states through an increased dependence on cell replication checkpoints that enable accurate DNA repair, scheduled mitotic entry, and survival (8, 12). When these key checkpoints are compromised, cancer cells undergo replication stress–driven mitotic catastrophe and death (13, 14). One critical cell cycle checkpoint regulator is the WEE1 kinase, which modulates CDK1 and CDK2 activity through direct inhibitory phosphorylation (15, 16). Functionally, phosphorylation at tyrosine 15 (Y15) on CDK1 by WEE1 delays progression at the $G_2$/M checkpoint (15, 17), restricting premature entry into mitosis. Thus, as part of a mechanism of adaptation to CCNE1-associated replication stress, WEE1 can enhance tumor cell survival. Through an integrative transcriptional and functional approach, we investigated how CIC-DUX4 sarcomas survive in a CCNE1-mediated high-replication-stress state through increased dependence on the WEE1 kinase. Moreover, we demonstrate that WEE1 is a therapeutic vulnerability in CIC-DUX4 sarcomas that can be targeted with clinically advanced WEE1 inhibitors.

**Authorship note:** RKMP and NJT contributed equally to this work.

**Conflict of interest:** The authors have declared that no conflict of interest exists.

**Copyright:** © 2022, Ponce et al. This is an open access article published under the terms of the Creative Commons Attribution 4.0 International License.

**Submitted:** June 15, 2021
**Accepted:** February 9, 2022
**Published:** March 22, 2022

**Reference information:** *JCI Insight*. 2022;7(6):e152293. https://doi.org/10.1172/jci.insight.152293.

## Results

Prior studies have identified cell cycle regulators as direct transcriptional targets of the CIC-DUX4 fusion oncoprotein (4, 18, 19). One key CIC-DUX4 transcriptional target is *CCNE1*, which regulates the $G_1$/S cell cycle transition (4, 20). CIC-DUX4–dependent *CCNE1* transcriptional upregulation compromises the $G_1$/S checkpoint and confers molecular and therapeutic dependence on the CCNE1/CDK2 complex (4). In order to identify additional actionable therapeutic targets in CIC-DUX4 sarcomas, we integrated CIC-DUX4–dependent gene expression changes with functional kinase activity screens in cells derived from patients with CIC-DUX4 sarcoma to identify candidate kinases that enable CIC-DUX4 survival (Figure 1A). Specifically, we performed comparative transcriptional analysis using a validated data set (GSE60740) comprising cells derived from patients with CIC-DUX4 sarcoma (IB120) with or without genetic silencing of CIC-DUX4 (19). Through a previously described approach in which IB120 cells with and without CIC-DUX4 expression were compared (4), we identified 165 putative CIC-DUX4–responsive genes, 43 of which contained the highly conserved CIC-binding motif (T[G/C]AATG[A/G]A) within –2 kb and +150 bp of the transcription start site (21) (see Methods for details). This analysis enabled us to identify high-confidence CIC-DUX4–dependent gene expression changes in cells endogenously expressing CIC-DUX4. In concordance with prior findings, we noted significant enrichment in genes that regulate the cell cycle, including $G_1$/S transition, mitosis, and cell cycle checkpoints (4). Genes that regulate DNA replication and chromosome segregation were also enriched in CIC-DUX4–replete cells compared with CIC-DUX4–KD cells (Figure 1B). In order to confirm these findings, we performed unbiased gene set enrichment analysis (GSEA) using 1426 up- and down-regulated genes identified upon CIC-DUX4 KD in IB120 (endogenous CIC-DUX4) cells (Supplemental Table 1; supplemental material available online with this article; https://doi.org/10.1172/jci.insight.152293DS1). This analysis consistently demonstrated enrichment of gene sets associated with $G_1$/S, mitosis, cell cycle checkpoints, and DNA replication (Figure 1C). These expression data indicated that cell cycle and DNA replication programs are key molecular targets of the CIC-DUX4 fusion oncoprotein. Next, we queried a publicly available data set that had been subjected to multiplex kinase activity (PamGene) profiling to identify active kinases in patient-derived CIC-DUX4 tumors, xenografts, and cell lines (22). Since our transcriptional analysis converged on genes involved in DNA replication, $G_1$/S transition, and mitosis, we focused on kinases that regulate the cell cycle in CIC-DUX4 sarcoma. Through a manual systematic analysis, we identified 20 unique phosphosites mapping to 14 independent kinases previously implicated in cell cycle regulation (Figure 1D) (22). Multiple CDK1 (4) and CDK2 (3) phosphosites were identified in our analysis, suggesting that these kinases have broad roles in CIC-DUX4 sarcoma cells. We noted that phosphosites mapping to the WEE1 kinase were highly repetitive and specific for the inhibitory phosphorylation site (Y15) on both CDK1 and CDK2, suggesting that CIC-DUX4 cells may depend on WEE1 activity to potentially delay $G_2$/M progression, and limit premature mitotic entry and mitotic catastrophe (Figure 1, E and F) (13, 15, 17). Consistent with this, we previously noted that ectopic expression of CIC-DUX4 leads to an increased $G_2$/M fraction in NIH 3T3 cells (4). Since CIC-DUX4 transcriptionally upregulates *CCNE1*, which can induce a high-replicative-stress state in cancer (5, 6, 9–11, 23), we hypothesized that WEE1 activity in CIC-DUX4 sarcomas may be an adaptive survival mechanism. To test whether WEE1 is necessary for CIC-DUX4 survival, we treated 2 independent patient-derived CIC-DUX4 cell lines (NCC_CDS1_X1_C1 and NCC_CDS2_C1) (22, 24) with the WEE1 inhibitor adavosertib (AZD1775) (25–28). Adavosertib treatment significantly decreased the viability of both NCC_CDS1_X1_C1 and NCC_CDS2_C1 cells as measured by CellTiter-Glo (CTG) and crystal violet assays (Figure 2, A–C). The decreased viability observed upon adavosertib treatment was associated with a decrease in CDK1 phosphorylation at Y15 and an increase in apoptosis as measured by poly(ADP-ribose) polymerase (PARP) cleavage in CIC-DUX4–expressing NCC_CDS_X1_C1 and NCC_CDS2_C1 cells. Moreover, we observed an increase in phosphorylation of serine 139 on the histone variant γH2AX, a sensitive marker of DNA damage, in adavosertib-treated compared with control cells (Figure 2, D and E) (29). Coupled with the enhanced caspase-3/7 activity observed upon adavosertib treatment, these findings indicate that pharmacologic inhibition of WEE1 induces apoptosis in CIC-DUX4 sarcoma cells, potentially through increased DNA damage and premature mitotic death (Figure 2, F and G). To further mitigate possible off-target effects of adavosertib, we performed genetic silencing of *WEE1* using 2 validated siRNAs (siWEE1-06 and siWEE1-08) that target independent regions of *WEE1* (30). Consistent with our pharmacologic findings, genetic inhibition of WEE1 decreased CDK1 Y15 phosphorylation and resulted in enhanced γH2AX expression and PARP cleavage compared with

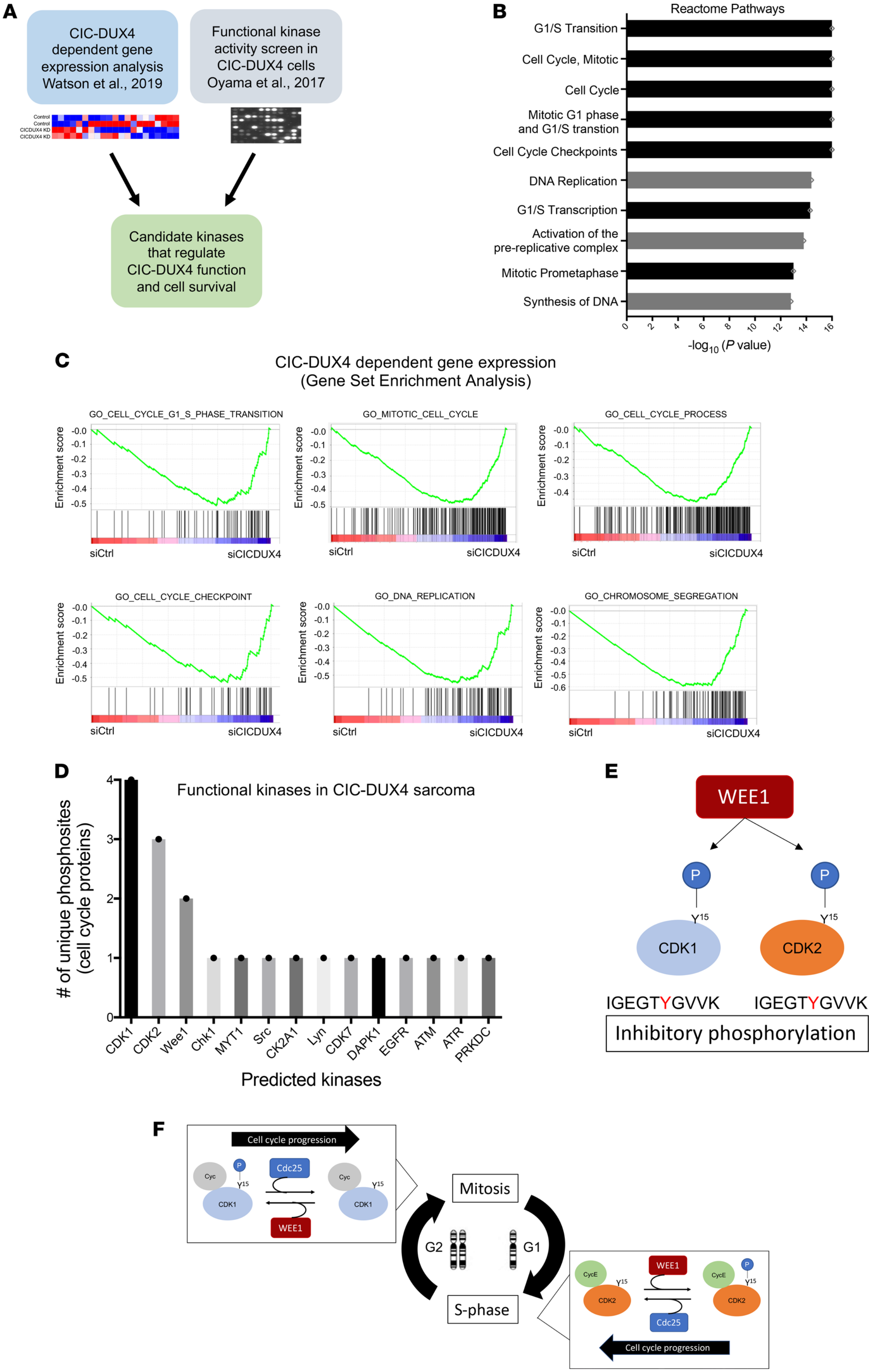
A
CIC-DUX4 dependent gene expression analysis Watson et al., 2019
Control
Control
CICDUX4 KD
CICDUX4 KD
Functional kinase activity screen in CIC-DUX4 cells Oyama et al., 2017
Candidate kinases that regulate CIC-DUX4 function and cell survival
B
Reactome Pathways
G1/S Transition
Cell Cycle, Mitotic
Cell Cycle
Mitotic G1 phase and G1/S transtion
Cell Cycle Checkpoints
DNA Replication
G1/S Transcription
Activation of the pre-replicative complex
Mitotic Prometaphase
Synthesis of DNA
0
2
4
6
8
10
12
14
16
-log10 (P value)
C
CIC-DUX4 dependent gene expression
(Gene Set Enrichment Analysis)
GO_CELL_CYCLE_G1_S_PHASE_TRANSITION
GO_MITOTIC_CELL_CYCLE
GO_CELL_CYCLE_PROCESS
GO_CELL_CYCLE_CHECKPOINT
GO_DNA_REPLICATION
GO_CHROMOSOME_SEGREGATION
Enrichment score
-0.0
-0.1
-0.2
-0.3
-0.4
-0.5
-0.6
siCtrl
siCICDUX4
D
Functional kinases in CIC-DUX4 sarcoma
# of unique phosphosites (cell cycle proteins)
0
1
2
3
4
CDK1
CDK2
Wee1
Chk1
MYT1
Src
CK2A1
Lyn
CDK7
DAPK1
EGFR
ATM
ATR
PRKDC
Predicted kinases
E
WEE1
P
P
Y15
Y15
CDK1
CDK2
IGEGTYGVVK
IGEGTYGVVK
Inhibitory phosphorylation
F
Cell cycle progression
Cyc
P
Y15
CDK1
Cdc25
WEE1
Cyc
Y15
CDK1
Mitosis
G2
G1
S-phase
CycE
Y15
CDK2
WEE1
Cdc25
CycE
P
Y15
CDK2
Cell cycle progression

**Figure 1. Integrative transcriptomic and kinase activity screen identifies WEE1 as a target in CIC-DUX4 sarcoma.** (**A**) Approach to identifying candidate kinases that regulate CIC-DUX4 sarcoma survival. Watson et al., 2019: ref. 19; Oyama et al., 2017: ref. 22. (**B**) Reactome pathway analysis identifies CIC-DUX4–dependent cell cycle and DNA replication pathways. (**C**) GSEA reveals cell cycle, DNA replication, and chromosome segregation at CIC-DUX4 targets. (**D**) PamGene array identifies functional kinases that regulate cell cycle and DNA replication in CIC-DUX4 cells. (**E**) Model of WEE1 inhibitory kinase motifs in CDK1 and CDK2. (**F**) Schematic of WEE1-regulated cell cycle control.

control (Figure 2, H and I). Moreover, genetic silencing of WEE1 decreased NCC_CDS1_X1_C1 and NCC_CDS2_C1 cell viability compared with control as measured by CTG assay (Figure 2, J and K) and crystal violet (Figure 2, L and M) assays. In contrast, we did not observe a decrease in the viability of A673 (Ewing sarcoma [ES], EWSR1-FLI1$^+$) or RH41 (alveolar rhabdomyosarcoma, PAX3-FOXO1$^+$) cells upon WEE1 KD compared with control (Supplemental Figure 1, A–D). In order to further demonstrate that the adavosertib-mediated apoptotic effect was dependent on CDK1 and/or CDK2, we silenced CDK1 and/or CDK2 in CIC-DUX4–expressing cells. We noted an increase in $IC_{50}$ with combinatorial CDK1 and CDK2 silencing relative to control or either CDK1 or CDK2 KD alone (Figure 2, N and O, and Supplemental Figure 2, A–F). In order to further link WEE1-mediated suppression of CDK1 activity to survival, we used the well-characterized CDK1 variant $CDK1^{AF}$ (31). The WEE1 inhibitory phosphosite in CDK1 (Y15) is replaced in $CDK1^{AF}$, generating a constitutively active isoform that is not responsive to WEE1 activity. Expression of this $CDK1^{AF}$ variant in NCC_CDS1_X1_C1 or NCC_CDS2_C1 cells decreased viability compared with control (Figure 2P). These findings indicate that WEE1 may promote CIC-DUX4 survival through inhibitory phosphorylation of CDK1. Through these studies, we reveal a pro-survival role for WEE1 and highlight a therapeutic vulnerability in CIC-DUX4 sarcomas.

Multiple preclinical studies have recently shown that in vitro efficacy of adavosertib does not directly translate into clinical responses to WEE1 inhibition in unselected patient populations. Importantly, increased *CCNE1* expression has been consistently correlated with clinical response to WEE1 inhibitors (32–37). Thus, *CCNE1* mRNA expression is a patient selection biomarker for WEE1 inhibitor response in patients with cancer at the clinical level. Therefore, in order to understand whether WEE1 inhibitor response is mechanistically linked to CCNE1 expression in CIC-DUX4–positive cell lines, we first knocked down *CCNE1* in NCC_CDS1_X1_C1 and NCC_CDS2_C1 cells and treated them with adavosertib. We observed decreased sensitivity to adavosertib in NCC_CDS2_C1 cells expressing si*CCNE1* compared with those expressing si*Control* (Figure 2Q). Moreover, since we previously noted a compensatory increase in *CCNE2* (>100-fold) expression in NCC_CDS1_X1_C1 cells upon *CCNE1* KD (4), we performed dual *CCNE1* and *CCNE2* KD in NCC_CDS1_X1_C1 cells; we consistently noted a decrease in adavosertib sensitivity, as demonstrated by $IC_{50}$ dose compared with control (Figure 2R). We did not observe a similar increase in adavosertib $IC_{50}$ dose or *CCNE2* mRNA expression in A673 (ES, EWSR1-FLI1$^+$) and RH41 (alveolar rhabdomyosarcoma, PAX3-FOXO1$^+$) cells upon *CCNE1* KD (Supplemental Figure 3, A–F). These findings indicated that the effect of the WEE1 inhibitor that we observed in NCC_CDS1_X1_C1 and NCC_CDS2_C1 cells was partially dependent on CCNE1/CCNE2 expression. Since CCNE1 expression is a clinically validated biomarker of WEE1 inhibitor response, we anticipate that individuals with CIC-DUX4 sarcomas, but not other small round blue cell tumors including ES or alveolar rhabdomyosarcoma, will benefit from WEE1 inhibitor treatment.

In certain cancers, increased CCNE1 expression (amplification or transcriptional upregulation) deregulates the cell cycle at the $G_1$/S and $G_2$/M checkpoints by accelerating S-phase entry and stimulating premature mitosis (5, 7, 9–11, 23). Moreover, a hyperactive CCNE1/CDK2 complex can increase DNA origin firing–inducing re-replication, leading to high DNA replication stress — a state that requires adaptive mechanisms at the cellular level to enable survival (38, 39). One response to this oncogene-induced replicative stress involves an increased dependence WEE1 (15, 16). Since CIC-DUX4 directly binds to the regulatory region of *CCNE1* to hyperactivate the CCNE1/CDK2 complex (4), we hypothesized that CIC-DUX4–mediated *CCNE1* upregulation induces DNA replication stress, stimulating DNA repair responses and thus sensitizing to WEE1 inhibition. To mechanistically dissect the role of WEE1 in limiting extensive DNA damage and premature mitotic entry, we first quantified γH2AX nuclear foci in NCC_CDS1_X1_C1 and NCC_CDS2_C1 cells through immunofluorescence (IF) staining following adavosertib treatment, as previously described (11). We noted an increased fraction of cells with a high degree of staining for nuclear γH2AX foci (>5 foci per cell) in adavosertib-treated compared with control cells (Figure 3, A and B). These findings indicated that WEE1 activity can limit DNA damage in CIC-DUX4 sarcomas. Since WEE1 inhibition

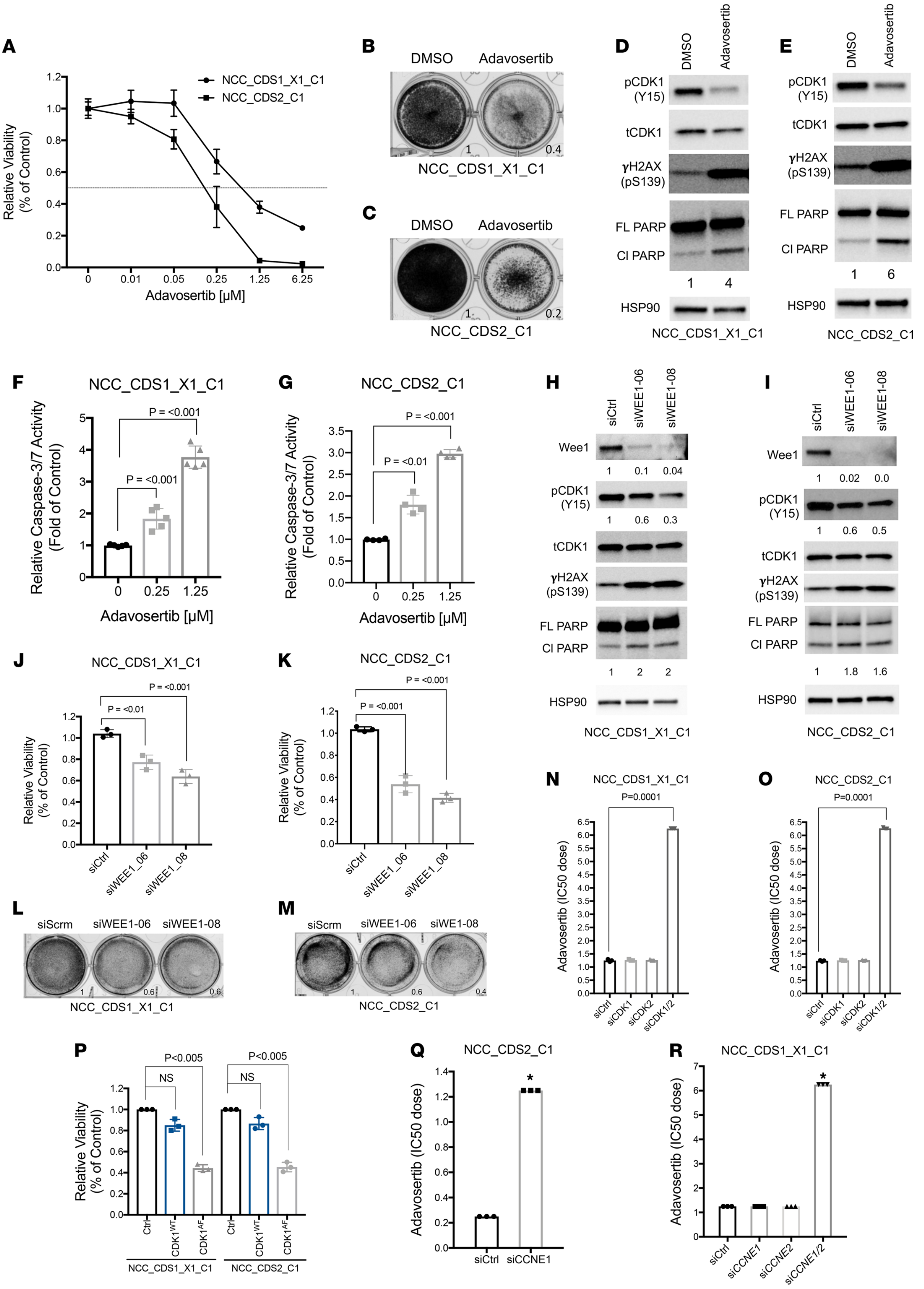
A
NCC_CDS1_X1_C1
NCC_CDS2_C1
Relative Viability (% of Control)
1.2
1.0
0.8
0.6
0.4
0.2
0.0
0
0.01
0.05
0.25
1.25
6.25
Adavosertib [μM]
B
DMSO
Adavosertib
1
0.4
NCC_CDS1_X1_C1
C
DMSO
Adavosertib
1
0.2
NCC_CDS2_C1
D
DMSO
Adavosertib
pCDK1 (Y15)
tCDK1
γH2AX (pS139)
FL PARP
Cl PARP
1
4
HSP90
NCC_CDS1_X1_C1
E
DMSO
Adavosertib
pCDK1 (Y15)
tCDK1
γH2AX (pS139)
FL PARP
Cl PARP
1
6
HSP90
NCC_CDS2_C1
F
NCC_CDS1_X1_C1
Relative Caspase-3/7 Activity (Fold of Control)
P = <0.001
P = <0.001
5
4
3
2
1
0
0
0.25
1.25
Adavosertib [μM]
G
NCC_CDS2_C1
Relative Caspase-3/7 Activity (Fold of Control)
P = <0.001
P = <0.01
3.5
3.0
2.5
2.0
1.5
1.0
0.5
0.0
0
0.25
1.25
Adavosertib [μM]
H
siCtrl
siWEE1-06
siWEE1-08
Wee1
1
0.1
0.04
pCDK1 (Y15)
1
0.6
0.3
tCDK1
γH2AX (pS139)
FL PARP
Cl PARP
1
2
2
HSP90
NCC_CDS1_X1_C1
I
siCtrl
siWEE1-06
siWEE1-08
Wee1
1
0.02
0.0
pCDK1 (Y15)
1
0.6
0.5
tCDK1
γH2AX (pS139)
FL PARP
Cl PARP
1
1.8
1.6
HSP90
NCC_CDS2_C1
J
NCC_CDS1_X1_C1
P = <0.001
P = <0.01
Relative Viability (% of Control)
1.2
1.0
0.8
0.6
0.4
0.2
0.0
siCtrl
siWEE1_06
siWEE1_08
K
NCC_CDS2_C1
P = <0.001
P = <0.001
Relative Viability (% of Control)
1.2
1.0
0.8
0.6
0.4
0.2
0.0
siCtrl
siWEE1_06
siWEE1_08
L
siScrm
siWEE1-06
siWEE1-08
1
0.6
0.6
NCC_CDS1_X1_C1
M
siScrm
siWEE1-06
siWE1-08
1
0.6
0.4
NCC_CDS2_C1
N
NCC_CDS1_X1_C1
P=0.0001
Adavosertib (IC50 dose)
6.5
6.0
5.5
5.0
4.5
4.0
3.5
3.0
2.5
2.0
1.5
1.0
0.5
0.0
siCtrl
siCDK1
siCDK2
siCDK1/2
O
NCC_CDS2_C1
P=0.0001
Adavosertib (IC50 dose)
6.5
6.0
5.5
5.0
4.5
4.0
3.5
3.0
2.5
2.0
1.5
1.0
0.5
0.0
siCtrl
siCDK1
siCDK2
siCDK1/2
P
P<0.005
NS
P<0.005
NS
Relative Viability (% of Control)
1.2
1.0
0.8
0.6
0.4
0.2
0.0
Ctrl
CDK1WT
CDK1AF
Ctrl
CDK1WT
CDK1AF
NCC_CDS1_X1_C1
NCC_CDS2_C1
Q
NCC_CDS2_C1
*
Adavosertib (IC50 dose)
1.4
1.2
1.0
0.8
0.6
0.4
0.2
0.0
siCtrl
siCCNE1
R
NCC_CDS1_X1_C1
*
Adavosertib (IC50 dose)
7
6
5
4
3
2
1
0
siCtrl
siCCNE1
siCCNE2
siCCNE1/2

**Figure 2. CIC-DUX4 sarcomas depend on WEE1 for survival.** (**A**) CTG viability assay of NCC_CDS1_X1_C1 and NCC_CDS2_C1 cells treated with adavosertib. Error bars represent SEM; performed in duplicate. Crystal violet assay of NCC_CDS1_X1_C1 (**B**) and NCC_CDS2_C1 (**C**) cells comparing adavosertib ($IC_{50}$ dose) and DMSO control. (**D**) Immunoblot analysis of NCC_CDS1_X1_C1 cells treated with adavosertib or DMSO control. Representative figure; performed in duplicate. Lysates were run on parallel gels. FL, full-length; Cl, cleaved. (**E**) Immunoblot analysis of NCC_CDS2_C1 cells treated with adavosertib or DMSO control. Representative figure; performed in duplicate. (**F** and **G**) Relative caspase-3/7 activity in NCC_CDS1_X1_C1 and NCC_CDS2_C1 cells treated with adavosertib versus control. One-way ANOVA; performed in triplicate. (**H** and **I**) Immunoblot analysis of NCC_CDS1_X1_C1 and NCC_CDS2_C1 cells expressing 2 independent WEE1 siRNAs. Representative figure; performed in duplicate. (**J** and **K**) CTG viability assay comparing 2 independent WEE1 siRNAs with scramble control in NCC_CDS1_X1_C1 and NCC_CDS2_C1 cells. One-way ANOVA; performed in triplicate. (**L** and **M**) Viability assay comparing 2 independent WEE1 siRNAs with scramble control (siScrm) in NCC_CDS1_X1_C1 and NCC_CDS2_C1 cells. One-way ANOVA; performed in duplicate. (**N** and **O**) Adavosertib $IC_{50}$ dose in NCC_CDS1_X1_C1 and NCC_CDS2_C1 cells expressing siCDK1, siCDK2, or siCDK1 and siCDK2. One-way ANOVA; performed in triplicate. (**P**) Relative viability comparing NCC_CDS1_X1_C1 and NCC_CDS2_C1 cells expressing $CDK1^{WT}$ or $CDK1^{AF}$ versus vector control. One-way ANOVA. Error bars represent SEM; performed in triplicate. (**Q**) Adavosertib $IC_{50}$ dose in NCC_CDS2_C1 cells expressing si*CCNE1* or siCtrl. Performed in triplicate. $^*P < 0.001$, Student's *t* test. (**R**) Adavosertib $IC_{50}$ dose in NCC_CDS1_X1_C1 cells expressing si*CCNE1*, si*CCNE2*, si*CCNE1*, and si*CCNE2* compared with siCtrl; performed in triplicate. $^*P < 0.001$, 1-way ANOVA.

with adavosertib induces premature mitotic entry and DNA damage (40, 41) in other cancer types, we next determined the effect of adavosertib on cell cycle progression in our patient-derived CIC-DUX4 sarcoma cells. Specifically, we analyzed the cell cycle distribution and γH2AX expression in NCC_CDS1_X1_C1 and NCC_CDS2_C1 cells in response to adavosertib treatment. Compared with control, adavosertib (0.5 μM at 48 hours) increased the $G_2/M$ fraction in our CIC-DUX4 cell lines (Figure 3, C–E and I–K, and Supplemental Figure 4, A and B), thus indicating premature mitotic entry and/or mitotic arrest that was associated with extensive DNA damage, as measured by increased γH2AX expression and an increase in the fraction of polyploid (>4N) cells (Figure 3, F–H and L–N, and Supplemental Figure 4, C–F). Consistent with our prior studies, we also observed an increase in the sub-$G_1$ fraction of adavosertib-treated compared with control cells (Supplemental Figure 4, C–F). Collectively, these findings demonstrate that WEE1 inhibition with adavosertib leads to premature mitosis, DNA damage, and apoptotic cell death.

CIC-DUX4 sarcomas are universally associated with poor clinical outcomes due to rapid metastatic progression and insensitivity to conventional chemotherapy agents (42). Thus, we next tested the translational impact of targeting the WEE1 kinase in preclinical models of CIC-DUX4 sarcoma. Specifically, we generated NCC_CDS1_X1_C1 and NCC_CDS2_C1 tumor xenografts in immunodeficient mice and treated them with adavosertib (100 mg/kg/d) and or vehicle control. In NCC_CDS1_X1_C1– and NCC_CDS2_C1–bearing mice, we noted tumor regression in the adavosertib compared with the vehicle-treated group (Figure 4, A and B, and Supplemental Figure 5, A–D). The overall objective response rates (≥30% reduction in tumor volume) to adavosertib in the NCC_CDS1_X1_C1 and NCC_CDS2_C1 cohorts were 87.5% (7 of 8) and 100% (6 of 6), respectively, without noted toxicity (Figure 4, C and D, and Supplemental Figure 6, A and B). Consistent with our in vitro data, NCC_CDS1_X1_C1 and NCC_CDS2_C1 tumor explants from adavosertib-treated mice demonstrated a decrease in CDK1 phosphorylation (Y15) and increased PARP cleavage compared with vehicle control (Figure 4, E and F). Immunohistochemical (IHC) analysis of NCC_CDS1_X1_C1 tumor explants further validated that WEE1 inhibition increased DNA damage and enhanced apoptosis, as demonstrated by increased γH2AX and cleaved caspase-3 expression in mice treated with adavosertib compared with vehicle control (Figure 4, G and H). To further assess the durability of the adavosertib response, we treated NCC_CDS1_X1_C1 tumor–bearing mice with adavosertib (100 mg/kg/d) for 24 days. Following initial tumor regressions, we observed prolonged tumor growth suppression (Figure 4I). These in vivo studies further validated WEE1 as a therapeutic vulnerability in CIC-DUX4 sarcomas that can be readily targeted through clinically advanced WEE1 inhibitors, including adavosertib (28, 35). Collectively, these data demonstrate a mechanism-based therapeutic strategy to precisely and effectively target CIC-DUX4 sarcomas in patients.

In this study, we employed an integrative transcriptional and functional approach to identify key clinically actionable vulnerabilities in CIC-DUX4 sarcoma. Through this analysis, we identified a WEE1-mediated adaptive response that enables CIC-DUX4 sarcoma survival by limiting massive DNA damage and mitotic catastrophe. These findings are in line with and expand our prior studies that reveal a dependence on CIC-DUX4–driven *CCNE1* expression in CIC-DUX4 sarcomas (4). Thus, we demonstrate that CIC-DUX4 sarcomas transcriptionally upregulate *CCNE1*, compromising the $G_1/S$ checkpoint and conferring dependence on WEE1 to limit DNA damage–associated cell death (Figure 4J). Importantly, these studies reveal a precision medicine–based therapy for CIC-DUX4 sarcomas, which remain an aggressive and lethal subset of human cancer.

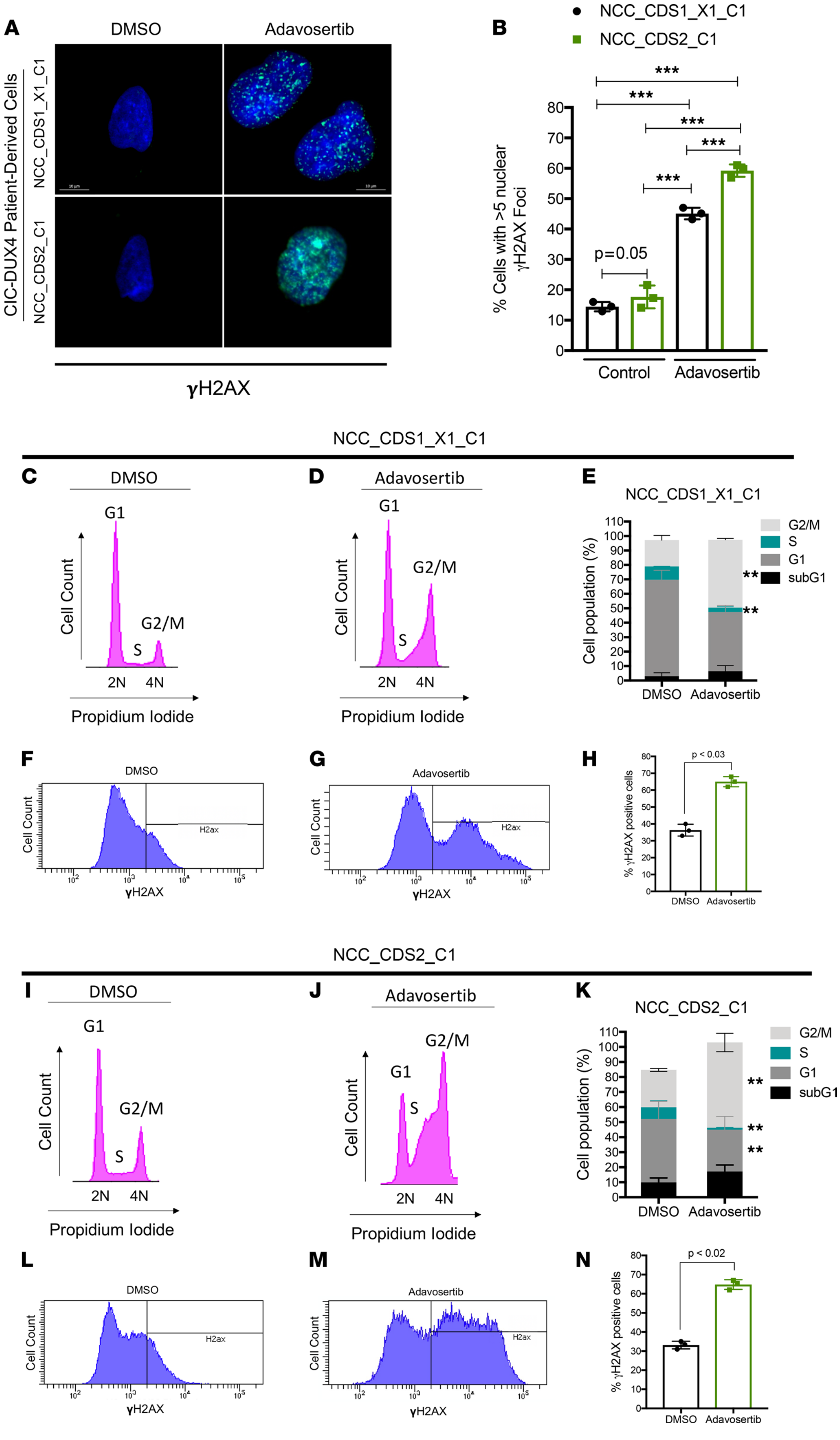

**Figure 3. WEE1 inhibition increases DNA damage and mitotic entry in CIC-DUX4 sarcoma cells.** (**A**) γH2AX IF staining of NCC_CDS1_X1_C1 and NCC_CDS2_C1 cells treated with adavosertib (0.5 μM) or DMSO (48 hours). Representative figure; performed in triplicate. Scale bars: 10 μm. (**B**) Quantitative analysis of γH2AX IF in **A** demonstrating the percentage of NCC_CDS1_X1_C1 or NCC_CDS2_C1 cells with more than 5 nuclear γH2AX foci following treatment with adavosertib or control. Mean percentage over 10 HPFs. ***$P < 0.001$, 1-way ANOVA. Representative cell cycle histograms (PI staining) of NCC_CDS1_X1_C1 (**C** and **D**) and NCC_CDS2_C1 (**I** and **J**) cells treated with adavosertib or DMSO (48 hours). Percentage of adavosertib- (0.5 μM) and DMSO-treated (48 hours) NCC_CDS1_X1_C1 (**E**) and NCC_CDS2_C1 (**K**) cells in sub-$G_1$, $G_1$, S, and $G_2$/M phases as identified in **C**, **D**, **I**, and **J**. **$P < 0.05$, 1-way ANOVA. Performed in triplicate. Error bars represent SEM. Values for each fraction of cells in sub-$G_1$, $G_1$, S, and $G_2$/M are provided in Supplemental Figure 4, A and B. γH2AX expression in NCC_CDS1_X1_C1 (**F** and **G**) and NCC_CDS2_C1 (**L** and **M**) cells treated with adavosertib or DMSO. Percentage of γH2AX-positive cells among NCC_CDS1_X1_C1 (**H**) and NCC_CDS2_C1 (**N**) cells analyzed in **F**, **G**, **L**, and **M**. Student's *t* test. Error bars represent SEM.

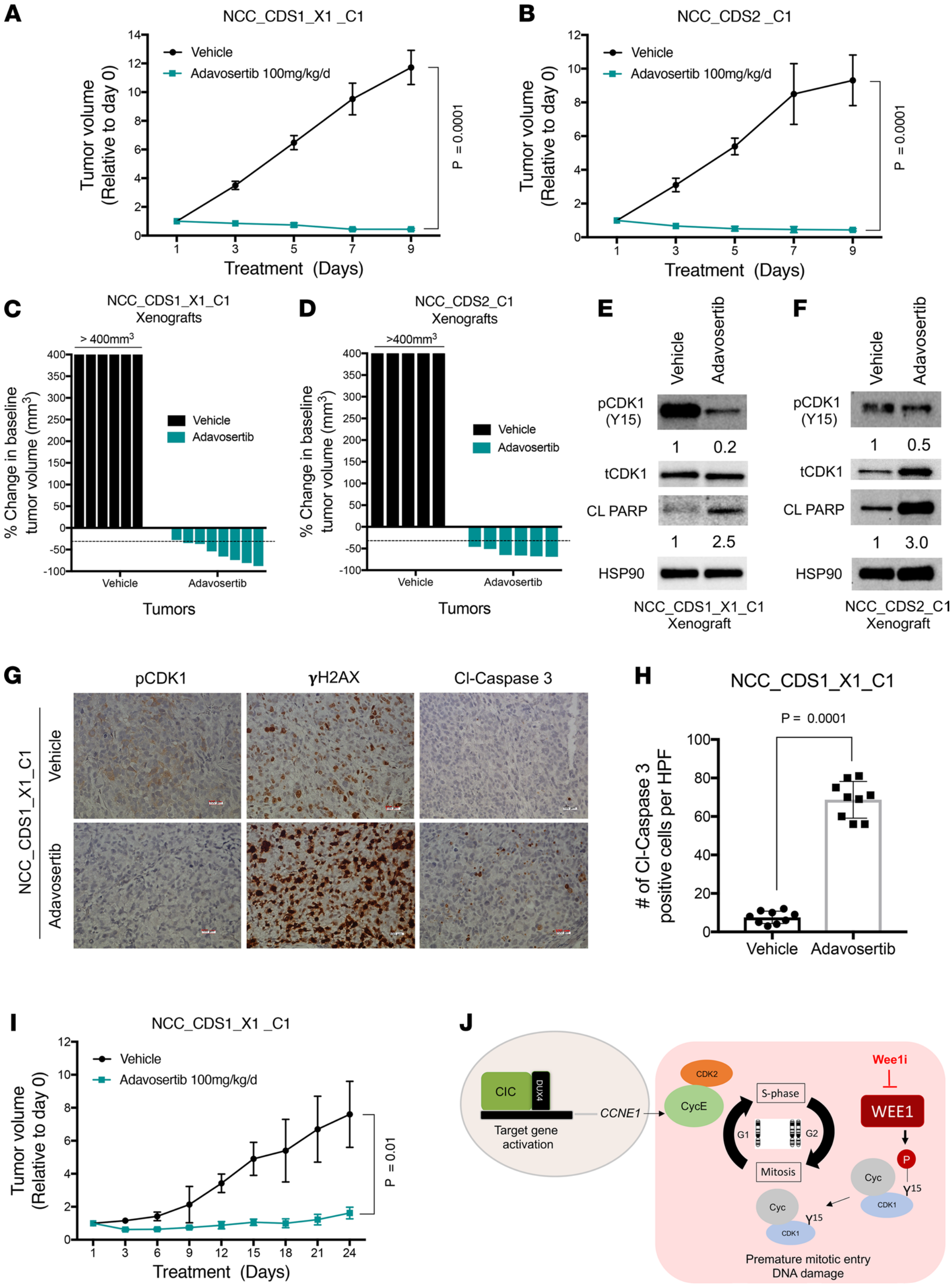

**Figure 4. WEE1 is a therapeutic target in CIC-DUX4 sarcomas.** Relative tumor volume of NCC_CDS1_X1_C1 (**A**) (*n* = 8 for adavosertib and *n* = 6 for vehicle control groups) and NCC_CDS2_C1 (**B**) (*n* = 6 for adavosertib and *n* = 5 for vehicle control groups) treated with adavosertib or vehicle control. Student's *t* test. Error bars represent SEM. (**C** and **D**) Percent change from baseline in tumor volume for NCC_CDS1_X1_C1 (*n* = 8 for adavosertib and *n* = 6 for vehicle control group) and NCC_CDS2_C1 (*n* = 6 for adavosertib and *n* = 5 for vehicle control) tumor–bearing mice in the adavosertib and vehicle cohorts. Percent change from baseline tumor volume for each mouse is shown in Supplemental Figure 5, C and D. (**E** and **F**) Immunoblot of NCC_CDS1_X1_C1 and NCC_CDS2_C1 tumor explants treated with adavosertib or vehicle control. (**G**) Representative IHC images of pCDK1, γH2AX, and cleaved caspase-3 in NCC_CDS1_X1_C1 tumor xenografts derived from mice treated with adavosertib or vehicle control. Scale bars: 100 μm. (**H**) Number of cleaved caspase-3–positive cells per HPF; 9 HPFs analyzed. Student's *t* test. (**I**) Tumor volume of NCC_CDS1_X1_C1 xenograft–bearing mice treated for 24 days with adavosertib (*n* = 6) compared with vehicle control (*n* = 6). (**J**) Model: CIC-DUX4–regulated *CCNE1* transcriptional upregulation leads to survival dependence on the $G_2$/M checkpoint kinase WEE1. Wee1i, WEE1 inhibition.

## Discussion

Through our studies we provide the initial translational framework for use of WEE1 inhibition as a therapeutic strategy in CIC-DUX4 sarcomas. Future studies should focus on rational combinatorial strategies to enhance DNA damage and potentially augment WEE1 inhibitor responses. Adavosertib is currently being evaluated in multiple tumor histologies and is proven safe as a monotherapy or in combination with other conventional targeted and chemotherapeutic agents as well as radiotherapy (11, 27, 28, 35). Importantly, our preclinical findings also illustrate how pharmacologic manipulation of key cell cycle regulators (CDK1 and/or CDK2) can potentially limit the efficacy of WEE1 inhibitors in cancer patients. With this caveat, adavosertib therapy is potentially a safe and efficacious therapy (28) that can be rapidly employed in the clinic to effectively target CIC-DUX4 sarcomas. Similarly, ZN-c3 (WEE1 inhibitor; Zentalis) is entering phase II studies as monotherapy and/or combination therapy in solid tumors, including sarcomas. One barrier in exploring the clinical response to WEE1 inhibitors in CIC-DUX4 patients is the relative rarity of CIC-DUX4 sarcomas (43). To overcome this obstacle, the sarcoma community must first differentiate CIC-DUX4 sarcomas as a unique entity and not routinely integrate them (clinically or pathologically) into more common small round cell sarcoma subtypes such as ES (4, 18, 20, 42, 44). This misrepresentation leads to a misconception that CIC-DUX4 sarcomas should be managed and treated with a strategy similar to that for ES (42, 45, 46). In most cases, ES-directed chemotherapy is not effective in CIC-DUX4 sarcomas (42). Thus, in order to advance the field, we must develop a more rational approach to treat this ultra-rare yet lethal subtype. Additionally, extensive collaboration is warranted to more rapidly identify and direct patients with CIC-DUX4 sarcoma to clinical trials that may be effective, such as WEE1 inhibitors (monotherapy or combination) or CDK2-directed therapies, as previously described (4). Finally, perhaps a reevaluation of clinical trial end points and a centralized clinical center for rare cancers would enhance clinical collaboration and accelerate therapeutic advancements (43).

## Methods

*Tumor xenografts*. Six- to eight-week-old female nude (NU/J) mice were purchased from the Jackson Laboratory. Specific pathogen–free conditions and facilities were approved by the American Association for Accreditation of Laboratory Animal Care. For subcutaneous xenotransplantation, $1.5 \times 10^6$ NCC_CDS1_X1_C1 and NCC_CDS2_C1 cells were resuspended in 50% PBS/50% Matrigel matrix and injected into the flanks of immunodeficient (NU/J) mice. Tumor-bearing mice were treated with either adavosertib or vehicle control for the designated time points.

*Cell lines and culture reagents*. NCC_CDS1_X1_C1 and NCC_CDS2_C1 were generated as patient-derived cell lines by a member of our research team (22, 24). The presence of the CIC-DUX4 fusion was confirmed in NCC_CDS1_X1_C1 and NCC_CDS2_C1 cells through RNA-Seq analysis using the "grep" command as previously described (47). NCC_CDS1_X1_C1 cells were maintained at 37°C in a humidified atmosphere at 5% $CO_2$ and grown in RPMI 1640 medium supplemented with 10% FBS, 100 IU/mL penicillin, and 100 μg/mL streptomycin. NCC_CDS2_C1 cells were cultured in RPMI medium supplemented with 10% FBS, 100 IU/mL penicillin, and 100 μg/mL streptomycin. Adavosertib (AZD1775, MK1775) was purchased from MedChemExpress (HY-10993).

*Gene KD and overexpression assays*. ON-TARGET scramble, WEE1 (WEE11-06-J-005050-06 and WEE1-08-J005050-08), CDK2 (L-003236-00-0005), CDK1 (L-003224-00-0005), CCNE1 (L-003213-00-0005), and CCNE2 (L-003214-00-0005) siRNAs were obtained from GE Dharmacon, and transfections were performed with DharmaFECT transfection reagent. CDK1 (catalog 61840) and $CDK1^{AF}$ (catalog 39872) plasmids were purchased from Addgene, and transfections were performed with FuGENE 6 transfection reagent.

*Western blot analysis*. All immunoblots represent at least 2 independent experiments. Adherent cells were washed and lysed with RIPA buffer supplemented with proteinase and phosphatase inhibitors. Proteins were separated by SDS-PAGE, transferred to nitrocellulose membranes, and blotted with Cell Signaling Technology (CST) antibodies recognizing HSP90 (CST 4874), total CDK1 (CST 9116), phosphorylated (Y15) CDK1 (CST 9111), WEE1 (CST 13084), PARP (CST 9542), total H2AX (CST 7631), and phosphorylated (S139) γH2AX (CST 9718).

*Real-time quantitative PCR*. Isolation and purification of RNA were performed using an RNeasy Mini Kit (QIAGEN). Total RNA (500 ng) was used in a reverse transcriptase reaction with the SuperScript III First-Strand Synthesis System (Invitrogen). Quantitative PCR included 3 replicates per cDNA sample.

Human CDK1, CDK2, CCNE1, CCNE2, and GAPDH were amplified with Taqman gene expression assays (Applied Biosystems). Expression data were acquired using an ABI Prism 7900HT Sequence Detection System (Applied Biosystems). Expression of each target was calculated using the $2^{-\Delta\Delta Ct}$ method, and mRNA levels are expressed relative to GAPDH.

*Xenograft tumor preparation for Western blot analysis*. Subcutaneous xenografts were explanted at the study end point and immediately immersed in liquid nitrogen and stored at –80°C. Tumors were disrupted with a mortar and pestle, followed by sonication in RIPA buffer supplemented with proteinase and phosphatase inhibitors. Proteins were separated as above. Antibodies to PARP, phosphorylated (Y15) CDK1, HSP90, and total CDK1 were purchased from CST.

*Xenograft tumor preparation for IHC staining*. Mice bearing NCC_CDS1_X1_C1 tumor xenografts were treated with 100 mg/kg adavosertib or vehicle control for 4 consecutive days. On day 4, tumors were explanted, fixed in 10% neutral buffered formalin for 72 hours, and embedded in paraffin, and sections of 5–10 μm were prepared. Sections were subsequently deparaffinized and incubated with antibodies directed against pCDK1 (CST 9111), γH2AX (CST 9718), and cleaved caspase-3 (CST 9661) overnight. Quantification of cleaved caspase-3 IHC staining was performed through analysis of at least 8 high-power fields (HPFs) per condition. Images were captured on a Zeiss Axioplan II microscope.

*Cell viability assays*. Cells were seeded overnight at a density of 3000 cells per well in 96-well plates and treated with relevant agents for 72 hours. Cell viability was determined using the CTG (Promega) assay according to the manufacturer's protocol. Each assay consisted of at least 3 replicate wells. For crystal violet assays, 100,000 cells were seeded per well in a 12-well plate (250,000 cells in a 6-well plate) and allowed to grow for 5 consecutive days. Cells were then fixed in 4% paraformaldehyde, followed by 0.05% crystal violet staining. Quantification was performed using ImageJ (NIH) software.

*Apoptosis assays*. Cells were seeded overnight at a density of 40,000 cells per well in 96-well plates and treated with relevant agents for 24 hours. Caspase-3/7 activity was measured on a Molecular Devices microplate reader using Caspase-Glo reagent per the manufacturer's protocol (Promega) and normalized to cell number.

*IF*. IF was performed on glass coverslips. Cells were fixed with 4% paraformaldehyde, quenched with 1× PBS and 10 mM glycine, and permeabilized with 0.1% Triton X-100, then incubated with conjugated (Alexa Fluor 488) phospho–histone H2A.X (S139) antibody (CST). ProLong Gold Antifade Mountant (Thermo Fisher Scientific) with DAPI was applied directly to fluorescently labeled cells on microscope slides. Fluorescence images were collected on a Zeiss Axioplan II fluorescence microscope.

*Cell cycle analysis*. To determine the effect of adavosertib (0.5 μm for 48 hours) on the cell cycle of NCC_CDS1_X1_C1 and NCC_CDS2_C1 cells, we first trypsinized them, washed with PBS plus 0.1% BSA, and fixed in ice-cold ethanol overnight. We subsequently treated them with RNase (CST) and stained with propidium iodide (PI) solution (Thermo Fisher Scientific) or with conjugated (Alexa Fluor 488) phospho–histone H2A.X (S139) antibody at room temperature for 30 minutes. Cells were analyzed on a BD LSR II flow cytometer.

*Pathway analysis and GSEA*. As previously described, 165 downregulated genes were identified in IB120 cells expressing siCtrl or siCIC-DUX4. 43 of 165 putative gene targets contained the CIC DNA-binding motif (T[G/C]AATG[A/G]A) within –2 kb and +150 bp of the transcription start site (4). These 43 high-confidence genes were analyzed using Reactome Pathway software (https://reactome.org/) to identify CIC-DUX4–regulated pathways. GSEA was performed using the top 1426 up-and downregulated genes in IB120 cells expressing siCIC-DUX4 versus control.

*Kinase array analysis*. As previously described, multiplex kinase activity profiling was performed in cells derived from patients with CIC-DUX4 sarcoma using PamGene technology and measured by PamStation according to the manufacturer's protocol (22). Manual identification of cell cycle kinases through the phosphorylation status of substrate peptides was performed using the data set published by Oyama et al. (22).

*Statistics*. Experimental data are presented as mean ± SEM. $P$ values derived for all in vitro and in vivo experiments were calculated using 2-tailed Student's $t$ test or 1-way ANOVA. A $P$ value less than 0.05 was considered significant.

*Study approval*. Tumor xenotransplantion and animal surgical procedures were reviewed and approved by the UCSF IACUC, protocol AN178670-03B

## Author contributions

RKMP and NJT designed and performed the experiments and analyzed the data. NQB analyzed the data and provided critical revisions on the manuscript. TK performed experiments and provided cell lines. RAO directed the project, analyzed experiments, and wrote the manuscript.

## Acknowledgments

RAO was supported by grants from the National Cancer Institute (K08CA222625 and R37CA255453), the Children's Cancer Research Fund, and the Sarcoma Foundation of America. NJT was supported by a Research Fellowship from the UCSF School of Medicine.

Address correspondence to: Ross A. Okimoto, University of California, San Francisco, 513 Parnassus Ave., HSW1201, San Francisco, California 94143, USA. Email: ross.okimoto@ucsf.edu.

---

1. Perry JA, et al. Biology and therapy of dominant fusion oncoproteins involving transcription factor and chromatin regulators in sarcomas. *Annu Rev Cancer Biol*. 2019;3(1):299–321.
2. Lin YK, et al. Negative MAPK-ERK regulation sustains CIC-DUX4 oncoprotein expression in undifferentiated sarcoma. *Proc Natl Acad Sci U S A*. 2020;117(34):20776–20784.
3. Yoshida H, et al. Accelerated degradation of PML-retinoic acid receptor alpha (PML-RARA) oncoprotein by all-trans-retinoic acid in acute promyelocytic leukemia: possible role of the proteasome pathway. *Cancer Res*. 1996;56(13):2945–2948.
4. Okimoto RA, et al. CIC-DUX4 oncoprotein drives sarcoma metastasis and tumorigenesis via distinct regulatory programs. *J Clin Invest*. 2019;129(8):3401–3406.
5. Fukuse T, et al. Prognostic significance of cyclin E overexpression in resected non-small cell lung cancer. *Cancer Res*. 2000;60(2):242–244.
6. Guerrero Llobet S, et al. Cyclin E expression is associated with high levels of replication stress in triple-negative breast cancer. *NPJ Breast Cancer*. 2020;6(1):40.
7. Bagheri-Yarmand R, et al. Cyclin E deregulation impairs mitotic progression through premature activation of Cdc25C. *Cancer Res*. 2010;70(12):5085–5095.
8. O'Connor MJ. Targeting the DNA damage response in cancer. *Mol Cell*. 2015;60(4):547–560.
9. Keck JM, et al. Cyclin E overexpression impairs progression through mitosis by inhibiting APC(Cdh1). *J Cell Biol*. 2007;178(3):371–385.
10. Resnitzky D, et al. Acceleration of the G1/S phase transition by expression of cyclins D1 and E with an inducible system. *Mol Cell Biol*. 1994;14(3):1669–1679.
11. Chen X, et al. Cyclin E overexpression sensitizes triple-negative breast cancer to Wee1 kinase inhibition. *Clin Cancer Res*. 2018;24(24):6594–6610.
12. Otto T, Sicinski P. Cell cycle proteins as promising targets in cancer therapy. *Nat Rev Cancer*. 2017;17(2):93–115.
13. Vitale I, et al. Mitotic catastrophe: a mechanism for avoiding genomic instability. *Nat Rev Mol Cell Biol*. 2011;12(6):385–392.
14. Fragkos M, Naim V. Rescue from replication stress during mitosis. *Cell Cycle*. 2017;16(7):613–633.
15. Di Rorà AGL, et al. A WEE1 family business: regulation of mitosis, cancer progression, and therapeutic target. *J Hematol Oncol*. 2020;13(1):126.
16. Matheson CJ, et al. Targeting WEE1 kinase in cancer. *Trends Pharmacol Sci*. 2016;37(10):872–881.
17. Parker LL, et al. p107wee1 is a dual-specificity kinase that phosphorylates p34cdc2 on tyrosine 15. *Proc Natl Acad Sci U S A*. 1992;89(7):2917–2921.
18. Yoshimoto T, et al. CIC-DUX4 induces small round cell sarcomas distinct from Ewing sarcoma. *Cancer Res*. 2017;77(11):2927–2937.
19. Watson S, et al. CIC-DUX4 expression drives the development of small round cell sarcoma in transgenic zebrafish: a new model revealing a role for ETV4 in CIC-mediated sarcomagenesis [preprint]. https://doi.org/10.1101/517722. Posted on bioRxov January 12, 2019.
20. Specht K, et al. Distinct transcriptional signature and immunoprofile of CIC-DUX4 fusion-positive round cell tumors compared to EWSR1-rearranged Ewing sarcomas: further evidence toward distinct pathologic entities. *Genes Chromosomes Cancer*. 2014;53(7):622–633.
21. Jimenez G, et al. The Capicua repressor--a general sensor of RTK signaling in development and disease. *J Cell Sci*. 2012;125(pt 6):1383–1391.
22. Oyama R, et al. Generation of novel patient-derived CIC-DUX4 sarcoma xenografts and cell lines. *Sci Rep*. 2017;7(1):4712.
23. Kok YP, et al. Overexpression of Cyclin E1 or Cdc25A leads to replication stress, mitotic aberrancies, and increased sensitivity to replication checkpoint inhibitors. *Oncogenesis*. 2020;9(10):88.
24. Yoshimatsu Y, et al. Establishment and characterization of NCC-CDS2-C1: a novel patient-derived cell line of CIC-DUX4 sarcoma. *Hum Cell*. 2020;33(2):427–436.
25. Hirai H, et al. Small-molecule inhibition of Wee1 kinase by MK-1775 selectively sensitizes p53-deficient tumor cells to DNA-damaging agents. *Mol Cancer Ther*. 2009;8(11):2992–3000.
26. Bridges KA, et al. MK-1775, a novel Wee1 kinase inhibitor, radiosensitizes p53-defective human tumor cells. *Clin Cancer Res*. 2011;17(17):5638–5648.
27. Zhang M, et al. WEE1 inhibition by MK1775 as a single-agent therapy inhibits ovarian cancer viability. *Oncol Lett*. 2017;14(3):3580–3586.
28. Takebe N, et al. Safety, anti-tumor activity, and biomarker analysis in a phase 1 trial of the once-daily Wee1 inhibitor adavosertib

(AZD1775) in patients with advanced solid tumors. *Clin Cancer Res*. 2021;27(14):3834–3844.

29. Bonner WM, et al. GammaH2AX and cancer. *Nat Rev Cancer*. 2008;8(12):957–967.
30. Pappano WN, et al. Genetic inhibition of the atypical kinase Wee1 selectively drives apoptosis of p53 inactive tumor cells. *BMC Cancer*. 2014;14(1):430.
31. Krek W, Nigg EA. Mutations of p34cdc2 phosphorylation sites induce premature mitotic events in HeLa cells: evidence for a double block to p34cdc2 kinase activation in vertebrates. *EMBO J*. 1991;10(11):3331–3341.
32. Takebe N, et al. Safety, antitumor activity, and biomarker analysis in a phase I trial of the once-daily Wee1 inhibitor adavosertib (AZD1775) in patients with advanced solid tumors. *Clin Cancer Res*. 2021;27(14):3834–3844.
33. Liu J, et al. ADAGIO: a phase IIb international study of the Wee1 inhibitor adavosertib in women with recurrent or persistent uterine serous carcinoma. *Int J Gynecol Cancer*. 2022;32(1):89–92.
34. Liu JF, et al. Phase II study of the WEE1 inhibitor adavosertib in recurrent uterine serous carcinoma. *J Clin Oncol*. 2021;39(14):1531–1539.
35. Lheureux S, et al. Adavosertib plus gemcitabine for platinum-resistant or platinum-refractory recurrent ovarian cancer: a double-blind, randomised, placebo-controlled, phase 2 trial. *Lancet*. 2021;397(10271):281–292.
36. Oza AM, et al. A Biomarker-enriched, randomized phase II trial of adavosertib (AZD1775) plus paclitaxel and carboplatin for women with platinum-sensitive TP53-mutant ovarian cancer. *Clin Cancer Res*. 2020;26(18):4767–4776.
37. Xu H, et al. CCNE1 copy number is a biomarker for response to combination WEE1-ATR inhibition in ovarian and endometrial cancer models. *Cell Rep Med*. 2021;2(9):100394.
38. Neelsen KJ, et al. Oncogenes induce genotoxic stress by mitotic processing of unusual replication intermediates. *J Cell Biol*. 2013;200(6):699–708.
39. Hills SA, Diffley JFX. DNA replication and oncogene-induced replicative stress. *Curr Biol*. 2014;24(10):R435–R444.
40. Kim H-Y, et al. Targeting the WEE1 kinase as a molecular targeted therapy for gastric cancer. *Oncotarget*. 2016;7(31):49902–49916.
41. Guertin AD, et al. Preclinical evaluation of the WEE1 inhibitor MK-1775 as single-agent anticancer therapy. *Mol Cancer Ther*. 2013;12(8):1442–1452.
42. Antonescu CR, et al. Sarcomas with CIC-rearrangements are a distinct pathologic entity with aggressive outcome: a clinicopathologic and molecular study of 115 cases. *Am J Surg Pathol*. 2017;41(7):941–949.
43. Blay J-Y, et al. The value of research collaborations and consortia in rare cancers. *Lancet Oncol*. 2016;17(2):e62–e69.
44. Watson S, et al. Transcriptomic definition of molecular subgroups of small round cell sarcomas. *J Pathol*. 2018;245(1):29–40.
45. Antonescu C. Round cell sarcomas beyond Ewing: emerging entities. *Histopathology*. 2014;64(1):26–37.
46. Mariño-Enríquez A, Fletcher CDM. Round cell sarcomas — biologically important refinements in subclassification. *Int J Biochem Cell Biol*. 2014;53:493–504.
47. Panagopoulos I, et al. The “grep” command but not FusionMap, FusionFinder or ChimeraScan captures the CIC-DUX4 fusion gene from whole transcriptome sequencing data on a small round cell tumor with t(4;19) (q35;q13). *PLoS One*. 2014;9(6):e99439.